

pubs.acs.org/Macromolecules Article

Two Stretching Regimes in the Elasticity of Bottlebrush Polymers

Sarit Dutta and Charles E. Sing*



Cite This: Macromolecules 2020, 53, 6946-6955



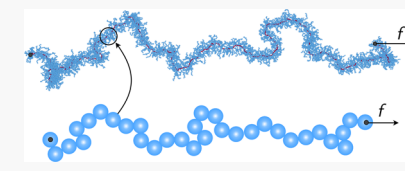
ACCESS

III Metrics & More



si Supporting Information

ABSTRACT: The elasticity of highly branched polymers, known as bottlebrush polymers, is integral to understanding their physical properties in a wide variety of applications; bottlebrush polymers undergo significant molecular extension in stretched, soft elastomers, in out-of-equilibrium environments during solution processing or in confinement-induced stretching. Unlike linear polymer chains where the molecular origin of this extension is well understood, it remains a challenge to connect molecular bottlebrush architecture to force-



extension behavior. In this paper, we present results from Monte Carlo simulations on bottlebrush polymers subjected to a constant pulling force and determine force-extension curves as a function of side-chain length. We show that different bottlebrush architectures exhibit a variety of force-extension behaviors. To understand bottlebrush elasticity, we compare with a parameterized wormlike cylinder implicit side chain model. This demonstrates the emergence of two distinct modes of bottlebrush stretching; at low forces, we demonstrate both linear and non-linear regimes corresponding to stretching the overall cylindrical shape of the molecule, and at high forces, there is specific extension of internal degrees of molecular freedom corresponding to the bottlebrush backbone. This two-regime molecular picture provides insight valuable to the molecular design of bottlebrush materials.

1. INTRODUCTION

Bottlebrush polymers are a class of branched polymers characterized by side chains densely grafted onto a linear backbone (see Figure 1a). Bottlebrush polymers have been intensely studied over the past two decades for applications in a wide range of novel functional materials, e.g., photonic²⁻⁴

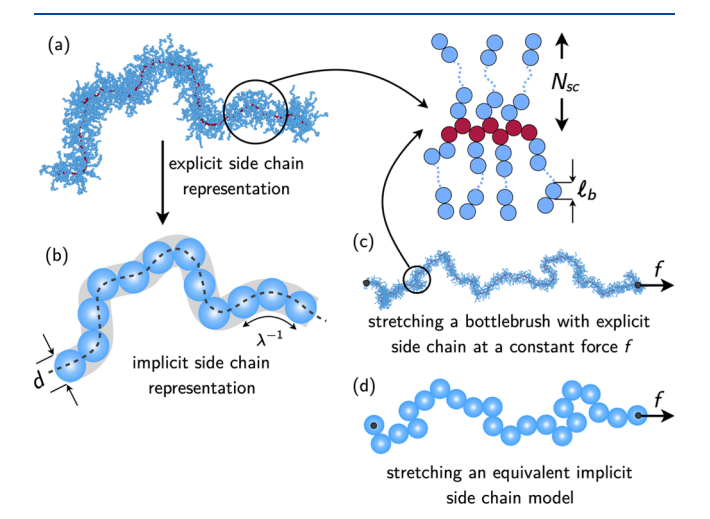


Figure 1. (a) Simulation snapshot of a bottlebrush polymer with explicit side chains with each side chain consisting of $N_{\rm sc}$ monomers, all monomers being of a size $I_{\rm b}$. (b) Schematic showing the implicit side chain representation of a bottlebrush polymer using a discrete wormlike cylinder with a Kuhn length λ^{-1} and width d. (c) Simulation snapshot of a stretched explicit side-chain bottlebrush under a pulling force f. (d) Schematic of a stretched conformation of an implicit side chain bottlebrush under the same pulling force f.

and phononic crystals, ⁵ molecular pressure sensors, ^{6,7} pressure sensitive adhesives, ⁸ pH-responsive surfaces, ⁹ stimuli-responsive molecular brushes, ¹⁰ and low-modulus elastomers capable of strain hardening and sustaining large deformation. The versatility of bottlebrush polymers stems from the molecular thickness and steric hindrance posed by the densely grafted side chains. The effects of these side chains on molecular conformations have been investigated in numerous works using scaling theories, ^{11–17} molecular simulations, ^{18–32} and scattering experiments. ^{33–42} The key insight gained from these studies is that the steric effect due to the side chains significantly increases the stiffness of bottlebrush molecules, imbuing them with a wormlike character and suppressing topological entanglements. ^{43–45} The consequent large dimensions and rapid dynamics, controlled by a large architectural design space, underlie the utility of this class of macromolecules.

Despite extensive fundamental investigation into connections between architecture and conformation in bottlebrush polymers, these efforts have largely focused on undeformed bottlebrush molecules, yet many applications for bottlebrush polymers utilize their elastic response for their functionality (e.g., sensors or elastomers), ^{7,46–50} which are deformed due to their assembly or confinement (e.g. photonic crystals, surfaces) ^{2–4,51–54} or stretch due to strong processing

Received: May 20, 2020 Revised: June 21, 2020 Published: August 3, 2020





flows.^{55–58} Indeed, recent efforts have demonstrated that the flow-induced stretching of bottlebrush polymers in solution can provide the foundation for advanced materials that can exhibit tunable structural color due to out-of-equilibrium behavior.^{4,57–59} There is thus a need to study the elasticity of bottlebrushes in solution and understand the molecular origin of force-extension relationships that govern material properties.

Only a few studies have considered bottlebrush stretching; Zhulina et al. 17 used a scaling approach, envisioning the bottlebrush as a string of superblobs of size D inspired by the approach of Birshtein et al. 11 Here, a superblob represents a length scale set by the side chains. Beyond the linear regime, their theory predicts two nonlinear power law regimes. 17 In the first regime, corresponding to lower forces f and smaller stretching distances R_x , the superblobs undergo a self-avoiding walk with Pincus-like scaling: 17,60

$$\frac{f}{k_{\rm B}T} \approx \frac{1}{D} \left(\frac{R_{\rm x}}{L^*}\right)^{3/2} \tag{1}$$

 L^* is an effective contour length based on the string of superblobs. In the second regime, corresponding to higher f, the backbone is stretched beyond the effective contour length, limiting to the result:¹⁷

$$\frac{f}{k_{\rm B}T} \approx \frac{1}{I_{\rm b}} \left(\frac{R_{\rm x}}{L}\right)^{\nu/1-\nu} \tag{2}$$

where L is the backbone contour length, $l_{\rm b}$ is the size of a segment, ν is the Flory exponent, and $k_{\rm B}T$ is the Boltzmann factor.

In addition to this theory, experimental studies on dsDNA bottlebrushes using optical tweezers by Rocha et al.⁶¹ showed evidence of scale-dependent stiffness in bottlebrushes. In the absence of an external force, the persistence length for dsDNA bottlebrushes was found to be ~95 nm⁶¹ based on fitting the end-to-end distances obtained from AFM images to the Marko-Siggia⁶² wormlike chain (WLC) formula, indicating considerable stiffening (the persistence length of bare dsDNA being ~50 nm). At high forces, however, fitting to the highforce WLC formula resulted in a considerable loss in stiffness (persistence length of $l_p \approx 15$ nm).⁶¹ This result is attributed to the extrinsic stiffness of bottlebrushes with the side-chain steric effect diminished at high forces. Further experimental evidence of scale-dependent stiffness comes from magnetic tweezer force spectroscopy by Saleh and co-workers. 63,64 For bottlebrushes of ssDNA backbones with poly(ethylene glycol) side chains and hyaluronan backbones with aggrecan side chains, a single value of l_p based on the WLC formula was insufficient to capture the force-extension behavior. Rather, following prior work on polyelectrolyte stretching, 65 they argue that the side chains induce an internal tension on the bottlebrush backbone that needs to be accounted for within the WLC formula; stiffness is again drastically reduced as the bottlebrush molecules is stretched. 63,64

Both theory and experiment thus suggest the presence of multiple regimes of bottlebrush stretching due to changes in the molecular architecture; however, there are limitations to their insights. The Zhulina theory assumes the realization of an asymptotic scaling limit, ¹⁷ which is well beyond the chain lengths accessible to synthetic chemists; ^{1,32,59,66} this is particularly true of the Pincus-regime, which is known to be challenging to observe in all but extremely long and flexible

polymer chains. $^{67-71}$ The experiments are limited by the use of bottlebrushes with lower grafting density and/or higher intrinsic backbone stiffness than most synthetic bottle-brushes. 61,63

Recently, we developed a parameterized bead-spring simulation model for bottlebrush polymers based on experimental data on bottlebrushes with a polynorbornene backbone and polylactic acid side chains under good solvent conditions.³² This model allows in silico exploration of architecture-conformation relationships in bottlebrush solutions over a wide range of architectural features (backbone and side chain lengths), including bottlebrushes with side chain length variations along the backbone and those exhibiting a persistent molecular shape.^{72.73} Since the side chains are explicitly resolved in this model, we call this model an explicit side chain (ESC) model. A simulation snapshot of a bottlebrush molecule with explicit side chains is shown in Figure 1a. Although the ESC model is well suited for investigating intramolecular details of a bottlebrush, reaching experimentally relevant lengths and time scales becomes computationally challenging. To overcome this problem, we developed a coarse-grained model of bottlebrushes that represents the side chains implicitly.⁷⁴ We will refer to this coarse-grained representation as an implicit side chain (ISC) model. The ISC model considers a bottlebrush molecule as a continuous wormlike cylinder, 36,38,40,75-81 parameterized by a contour length L^* , thickness d, Kuhn length λ^{-1} , and an excluded volume parameter B. These parameters can be determined from simulations using the ESC model.⁷⁴ This continuous cylinder is represented as a sequence of touching hard spheres of a diameter d_1^{74} as shown in Figure 1b. The ISC model enables rapid simulation of bottlebrushes that is faster than that of ESC models by orders of magnitude.

In this paper, we bridge the gap between asymptotic scaling theories and experimental measurements by providing insight through computationally studying the effect of a stretching force on a bottlebrush polymer and rationalizing these observations within the framework of the ISC model. Comparison between implicit and explicit side chain simulations elucidate two distinct regimes of bottlebrush stretching, corresponding to the coarse-graining length scales and providing insight into the suitability of the ISC model in out-of-equilibrium or stretched scenarios. At low forces, we show that the ISC model is sufficient to explain bottlebrush stretching as the overall cylindrical structure of the bottlebrush is extended. At high forces, however, internal backbone degrees of freedom begin to be extended leading to a failure of the ISC model prediction.

2. BOTTLEBRUSH MODEL AND SIMULATION METHOD

We use two different models for bottlebrush polymers to study their force-extension behavior: (i) a tangent hard sphere model²⁰ resolving the backbone as well as all side chains, referred to as the explicit side chain (ESC) model, and (ii) a discrete wormlike cylinder (dWLCy) model that treats the side chains implicitly via the cylinder thickness, referred to as the implicit side chain (ISC) model. In the following, we describe each model and the methodological details pertaining to simulations based on that model.

For simulations with the ESC model, the backbone degree of polymerization is held fixed at $N_{\rm bb}$ = 926 beads with each bead being connected to a side chain consisting of $N_{\rm sc}$ beads,

resulting in a bottlebrush with a grafting density of one side chain per backbone monomer. The side chain length is varied from $N_{sc} = 0$ to 20 with $N_{sc} = 0$ simply being a linear chain. All backbone and side chain beads are tangent hard spheres, each of a radius a, resulting in a purely repulsive bead-bead interaction representative of an athermal solvent. The bond length $l_b = 2a$ is constant for all cases. The bead at one end of the backbone is held fixed at the origin of the simulation coordinate system, while a constant force f is applied at the other end along the positive x direction, as shown in Figure 1c. f is given in units of k_BT/l_B , such that $fl_B/k_BT=1$ is approximately 6.1 pN based on the parameterization in our prior work.³² We verified (see Figure S1 in the Supporting Information) that tethering one end does not change the forceextension behavior by comparing to simulation results where both ends are allowed to fluctuate.

Equilibrium conformations corresponding to the constant-force ensemble are sampled for each value of f using the Metropolis Monte Carlo (MC) method with a backbone pivot, side chain crankshaft, and side chain end-rotation moves. The side chains in our simulations are short compared to the backbone, so the relaxation of side chains, even using a simple crankshaft and end rotation, occurs much faster than that of the backbone. The effect of the pulling force is accounted for by an energetic contribution, $U_f = \mathbf{R} \cdot f \hat{\mathbf{x}}$ where \mathbf{R} is the backbone end-to-end vector. Initial conformations are generated by relaxing from a fully extended conformation and setting f = 0.

Sampling is performed in blocks of 2000 MC cycles. Each MC cycle consists of a backbone pivot move, $N_{\rm sc}N_{\rm bb}$ crankshaft moves, and $N_{\rm bb}$ end rotation moves. The crankshaft and endrotation moves are performed only on the side chains. The block size depends on N_{sc} and f; low values of f require more blocks to obtain good averages and so do high values of N_{sc} due to a lower acceptance rate of the pivot move. Typically 10³-10⁵ blocks were found to be sufficient for data with a reasonable sampling error. For each value of f, 6-24 trajectories were generated depending on the relative magnitude of statistical fluctuations. The relative extension was calculated from the sampled conformations as $\langle \mathbf{R} \cdot \hat{\mathbf{x}} \rangle / L$ where $L = l_b(N_{bb} - 1) = 2a(N_{bb} - 1)$. We note that our simulations are representative of typical backbone lengths utilized in experimental studies with longer bottlebrushes exhibiting significant polydispersity for common chemistries such as polynorbornene-g-polylactide and polynorbornene-gpolystyrene.^{32,72} We also note that this simulation model has been directly compared to experiments and can quantitatively predict intrinsic viscosity for a wide variety of architec-

ISC models use a wormlike cylinder parameterization determined in our previous work⁷⁴ where the derivation of this model and its parameterization from the ESC simulations are described in detail. Here, we briefly recall the salient points: The ISC model is a discretized version of a continuous wormlike cylinder (WLCy), characterized by a contour length L^* , a thickness d, a Kuhn length λ^{-1} , and an excluded volume parameter B determined based on the quasi-two parameter theory by Yamakawa and co-workers. B is a measure of the excluded volume strength with dimensions of length defined as $B = \beta/(\Delta s)^2$ where Δs is the distance between two points on the chain contour and β is the binary cluster integral. Furthermore, if u(r) is the potential of the mean force between two segments, $\beta = 4\pi \int_0^\infty [1 - \exp{\{-u(r)/k_B T\}}]r^2 dr$.

The abovementioned parameters are determined by systematically fitting the end-to-end distance and radius of gyration calculated using the ESC model in the absence of a pulling force with appropriate analytical expressions. The contour length $L^* = m_L(N_{\rm bb} - 1)$ is taken to be proportional to the number of bonds with the proportionality constant representing the relative shortening of the contour due to crumpling of the bottlebrush backbone inside the cylinder. 20,83,84 First, we perform fits to the end-to-end distance data to obtain three parameters: the Kuhn length λ^{-1} , the contour length proportionality factor m_I , and the excluded volume parameter B. Second, we use the values of these three parameters to make a further one-parameter fit to the radius of gyration data to obtain the diameter d. d significantly captures the deviation of the ESC radius of gyration from that of an equivalent linear Kratky-Porod chain and has been found to be numerically close to 4 times the radius of gyration of the side chain.⁷⁴ The variable d is thus a direct conformational measure from simulation, which we distinguish from the scaling length scale D used by Zhulina et al. 17 despite their similar physical meanings. This completes the determination of the four fitting parameters. Third, we use the parameters so determined to perform a self-consistent check with data for the hydrodynamic radius and intrinsic viscosity using the analytical expressions provided for these quantities by Yamakawa and Yoshizaki.8

These parameters are listed in Table 1. Note that, for $N_{\rm sc} > 8$, B cannot be extracted from the fitting procedure as the

Table 1. Fitting Parameters for the WLCy Model

$N_{ m sc}$	m_L/a	λ^{-1}/a	d/a	B/a
2	1.252	20.83	5.77	11.06
4	1.228	33.90	8.60	18.83
8	1.223	62.11	13.15	30.53
14	1.209	117.6	18.93	
20	1.225	175.44	23.90	

molecule is not long enough compared to the Kuhn length; in such cases, the excluded volume is expected to play a minor role. These parameters provide accurate predictions for other single-chain quantities such as the hydrodynamic radius 40,74,81,85 and intrinsic viscosity $^{40,74-76,79,81}$ and reflect the shape of the bottlebrush polymer. The note that, for the high-grafting-density bottlebrushes considered in here and in the previous manuscript, the side-chain length governs the increases in the bottlebrush diameter d and even larger (i.e., non-linear with respect to d) increases in the Kuhn length λ^{-1} .

The ISC model is implemented as a chain of tangent hard spheres augmented with bending interactions between successive bonds. The discretized chain consists of L/d beads, each a tangent hard sphere of diameter d. The bending interaction $U_{\rm b}$ between successive bonds is of the form $U_{\rm b}/k_{\rm B}T=k_{\rm b}(1-\cos\theta)$ where $k_{\rm b}$ is the bending constant and θ is the complementary bond angle. The bending constant is related to the Kuhn length λ^{-1} through 86,87

$$\frac{\lambda^{-1}}{d} = \frac{k_{\rm b} - 1 + k_{\rm b} \coth k_{\rm b}}{k_{\rm b} + 1 - k_{\rm b} \coth k_{\rm b}} \tag{3}$$

The generation of the initial conformation and sampling at different values of the pulling force *f* follow the same protocol as described for the ESC model, except that the pivot, crankshaft, and end-rotation MC moves act on all the bonds of

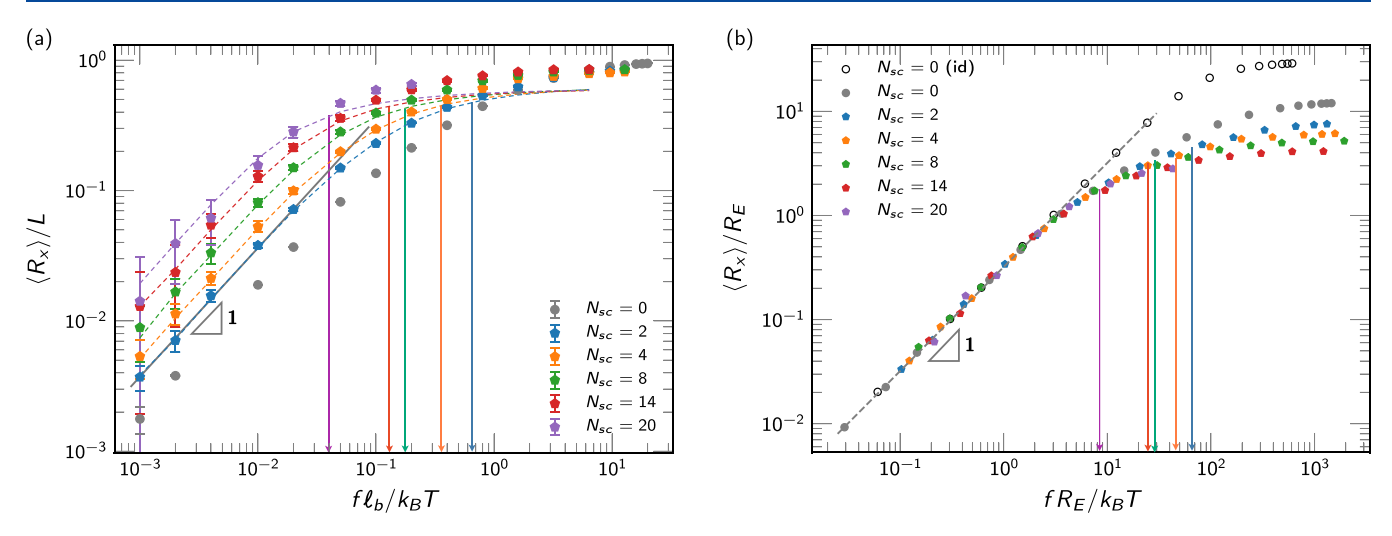


Figure 2. (a) Force-extension curves for bottlebrush polymers for different values of side chain lengths, $N_{\rm sc}$. A linear chain is denoted as $N_{\rm sc}=0$. Markers denote results determined using an explicit side chain model, while dashed lines indicate data obtained using an implicit side chain model. For all side chain lengths, the implicit and explicit model predictions deviate beyond a certain force f^{**} . The vertical lines (also appropriately denoted in (b)) indicate estimates of f^{**} obtained based on backbone stretching on the length scale of the coarse-grained beads in the implicit side chain model. (b) At low forces, the relative extension for all side chains [including an ideal chain, indicated by $N_{\rm sc}=0$ (id)] collapses onto a single curve, showing a linear scaling in force. While different values of $N_{\rm sc}$ deviate beyond this linear regime, the ISC remains valid (i.e., forces are lower than the vertical lines for a given $N_{\rm sc}/N_{\rm sc}$) well into the non-linear regime.

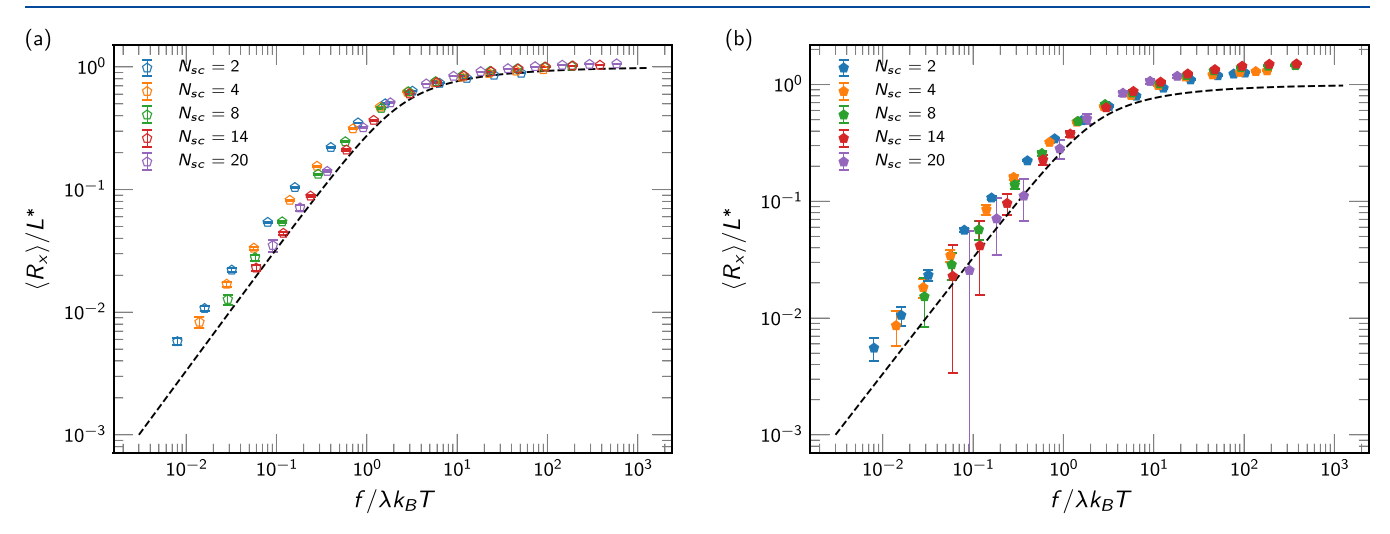


Figure 3. (a) Force-extension data obtained using the ISC model for different values of the side chain length $N_{\rm sc}$. The contour length is denoted by L^* to explicitly indicate that the length is that of the underlying wormlike cylinder. (b) Force-extension data obtained using the ESC model, but the relative extension is with respect to L^* . The dashed line in both panels denotes the Marko-Siggia prediction⁶² for an ideal semiflexible chain. The data in (a) deviates from the Marko-Siggia curve due to the presence of excluded volume effects in the data with the deviation progressively diminishing for higher $N_{\rm sc}$ values. The data in (b) further deviates from the Marko-Siggia prediction at a large f, which we attribute to the extension of local backbone degrees of freedom. This results in a fractional extension greater than 1 in this limit, precluding observance of the high-force nonlinear behavior embodied in the Marko-Siggia formula.

the chain. A simulation snapshot of a stretched bottlebrush molecule represented by the ISC model is shown in Figure 1d.

3. RESULTS AND DISCUSSION

Figure 2a shows a double logarithmic plot of the force-extension curves for several values of $N_{\rm sc} \leq 20$, including that of the linear chain $(N_{\rm sc}=0)$. Here, the extension $\langle R_x \rangle$ is normalized by the fully stretched contour length $L=l_{\rm b}(N_{\rm bb}-1)$ and the force f is normalized using the thermal energy $k_{\rm B}T$ and the bond length $l_{\rm b}$. As expected, at a small $\langle R_x \rangle$ and f, the slope of one indicates Hookean stretching for all bottlebrush polymers. However, the vertical shift of these curves with increasing $N_{\rm sc}$ reflects the increasing molecular rigidity due to

the side chain steric interactions; this decrease in the modulus is due to the decreased conformational entropy of these increasingly stiff bottlebrush chains. The finite extensibility of these molecules approaches the expected normalized extension $\frac{\langle R_x \rangle}{L} = 1$. Figure 2b shows that, at low forces, the relative extension collapses for all values of $N_{\rm sc}$ when the reference length scale is set at the end-to-end distance R_E , normalizing the conformational changes due to the side-chain-altered persistence lengths for the bottlebrush polymers. This is even true for ideal chains (open symbols) where the excluded volume is completely removed in the MC simulations. The rescaling in Figure 2b breaks down for higher forces as simply rescaling the force does not lead to a collapse for side chain

lengths, reflecting the emergence of new length scales separate from the equilibrium bottlebrush polymer dimensions.

To gain insight into the nature of the different regimes, we invoke the implicit (ISC) description of a bottlebrush polymer, which coarse-grains the sub-d molecular details that captures, e.g., side chain degrees of freedom. The state of the coarse-grained model is parameterized from equilibrium bottlebrush conformations in dilute solution, we expect a low-force limiting extension behavior similar to the full explicit side-chain representation. Indeed, we show that there is agreement for the linear regime by plotting the results of the ISC model in Figure 2a. However, this agreement remains quantitative for all values of $N_{\rm sc}$ even beyond the linear regime. This agreement is most apparent for small $N_{\rm sc}$ where the initial change in the slope associated with finite extensibility is also captured by the ISC model; however, this occurs for all values of $N_{\rm sc}$ considered in this manuscript.

The ISC model has already been shown to be a good descriptor of large-scale static and dynamic properties of single bottlebrushes in the absence of a pulling force, 74 and it is useful here to consider the range of applicability of this model for the same bottlebrush molecules when force is applied. By construction, the ISC model should reproduce the behavior characteristic of a wormlike chain. In Figure 3a, we compare the ISC data with the prediction from the Marko-Siggia (MS) interpolation formula of for a wormlike chain, showing excellent agreement. There is some deviation from the MS formula due to the presence of excluded-volume effects in our simulation, which are absent in the MS expression. This deviation decreases with an increase in N_{sc} , reflecting the reduced role of the excluded volume compared to bottlebrush stiffness in governing its relative extension. Therefore, both the linear and weakly non-linear force-extension behavior of bottlebrush polymers can be well described by parameterizing the MS force-extension expression with the ISC parameters. The connection of these ISC parameters to the molecular bottlebrush architecture has been studied previously,⁷⁴ and it is thus straightforward to account for the molecular weight, grafting density, and side-chain length effects.

However, for all values of N_{sc} there is a critical force (indicated with vertical lines calculated later in the paper) above which the ISC model deviates from the ESC calculations. Here, the explicit model stretches further than the implicit model, representing extension of the internal backbone degrees of freedom not resolved in the ISC. This can be seen in both Figure 2a where we directly compare the ISC and ESC model data and in Figure 3b where we compare the ESC model data with the MS formula. In the latter plot, the contour length of the wormlike cylinder L^* is used to normalize the extension. While the data is indicative of collapsing onto a single curve, the fractional extension for the bottlebrush polymers deviates significantly at high forces and often exceeds a fractional extension of $\frac{\langle R_x \rangle}{L^*} = 1$. This indicates that the bottlebrush molecule does not follow the high-force nonlinear behavior described by the MS formula for wormlike chains and the molecule is stretched beyond the wormlike cylinder contour of the unextended bottlebrush.

Our results thus suggest the existence of two distinct regimes of bottlebrush stretching, which we distinguish by the ability to capture the relative extension data with the ISC model; at low forces, the ISC model captures the molecular shape via the minimal wormlike cylinder parameters (i.e., width d, Kuhn

length λ^{-1} , and length L^*), and it is this structure that is stretched, first linearly and then non-linearly. At high forces, the bottlebrush backbone itself becomes stretched, allowing the explicit model to stretch beyond the implicit model (see Figure 4 for a schematic illustration). This is due to the



Low force: Backbone enclosed within implicit cylinder



High force: Backbone stretched beyond the implicit cylinder

Figure 4. Schematic showing backbone conformations under low and high pulling forces relative to the implicit cylinder. At a low force, extension of the implicit cylinder follows Marko—Siggia behavior due to side-chain-induced semiflexibility. At a high force, however, local backbone degrees of freedom are extended. This leads to an increase in the overall contour length of the cylindrical bottlebrush structure.

wormlike cylinder parameterization for which the contour length of the cylinder L^* is significantly less than the backbone contour length L due to the backbone exhibiting local conformational fluctuations. The high-force regime begins to stretch these local fluctuations, consistent with the backbone stretching regime predicted by Zhulina et al. However, in contrast to the predictions of Zhulina et al., this occurs without significant change in the nature of the side-chain interactions. We demonstrate this by plotting (see Figure S6 in the Supporting Information) the number of contacts $\langle N_C \rangle$ for a side-chain monomer with side-chain Δs backbone monomers away. Our simulations only exhibit small changes in these side-chain interactions.

As another point of contrast, we do not observe a Pincus-like scaling regime (see eq 1) in our simulations (see Figure S4). Note that the scaling regime predicted by Zhulina et al. ¹⁷ for the highly stretched polymers (see eq 2) yields the same power law exponent as eq 1 for athermal solutions ($\nu = 3/5$) with bottlebrushes having a side chain grafted to every backbone monomer (i.e., the spacer length is the same as the backbone bond length). We attribute this to the short (i.e., not at the asymptotic scaling limit) length of bottlebrush structures where excluded-volume interactions between locations along the wormlike cylinder structure play a small and often negligible role.90 The Pincus regime has been observed in stretching experiments on ssDNA, 68 and it is reasonable to expect that a similar regime will be observed for sufficiently long bottlebrushes as well. Prior work⁶⁹ on semiflexible chains indicates that the chain length must be more than λ^{-1} by over four decades to properly resolve the different regimes on a double-logarithmic force-extension plot with the Pincus regime observed for flexible chains with $N_{\rm bb}$ > 6400 in simulation studies. 69,71 To estimate how long our bottlebrushes would need to be, we modify this inequality with the Kuhn length $N_{\rm bb}\lambda \approx O(10^4)$, suggesting that, for a typical $\lambda^{-1} \approx 100$, a bottlebrush would need to have $N_{\rm bb} \approx O(10^6)$ to exhibit Pincus-like scaling. Consistent with our simulation observations, this is significantly longer than what is computationally

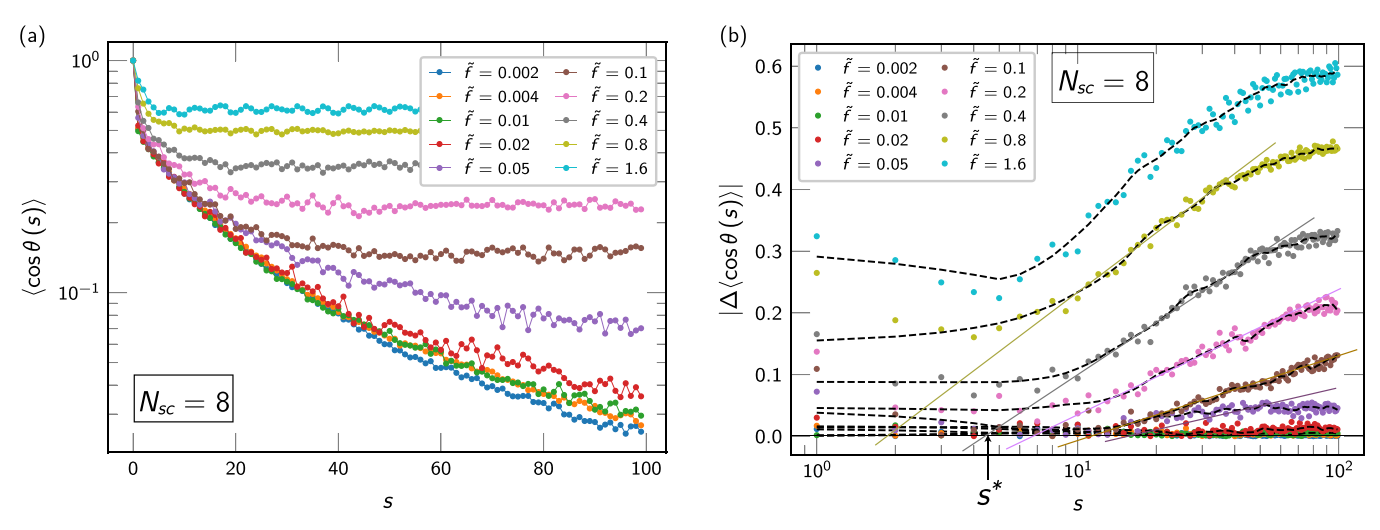


Figure 5. (a) Backbone bond—bond autocorrelation as a function of pulling force for $N_{\rm sc}=8$. (b) Deviation of the bond—bond autocorrelation function from their respective no-force values for the bottlebrush backbone at $N_{\rm sc}=8$ for different values of the pulling force; $\tilde{f}=fl_{\rm b}/k_{\rm B}T$. Dashed lines are meant to show the trend in the data to guide the eye. The intersection of the solid lines with zero marks the length scale s^* denoting the degree of stretching of the backbone.

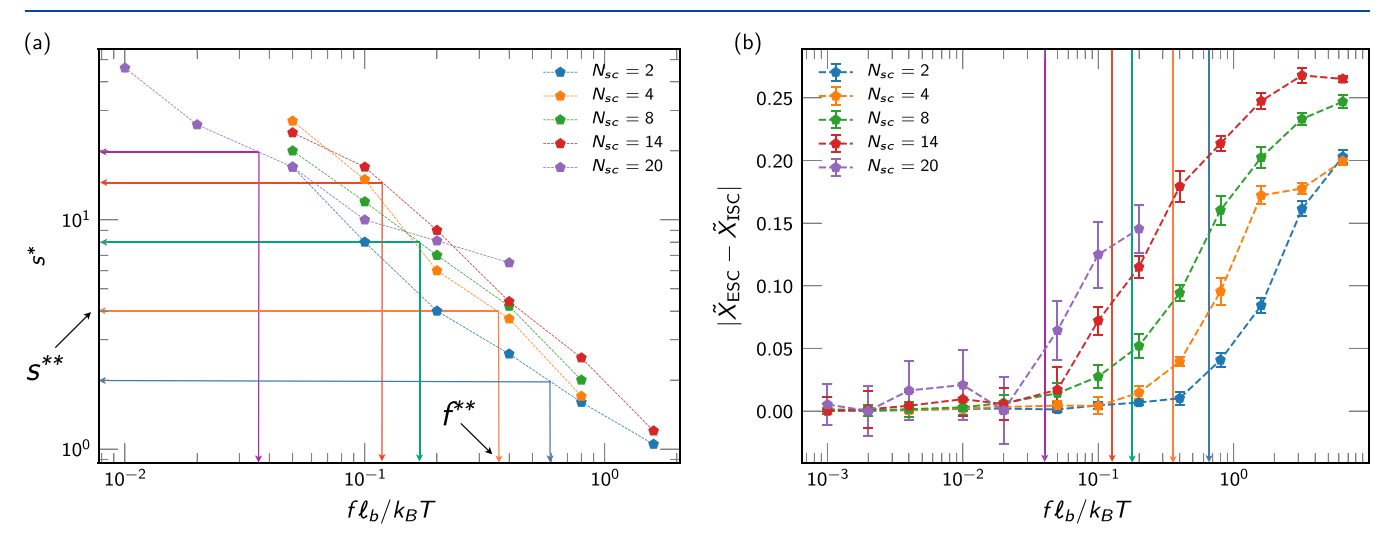


Figure 6. (a) s^* vs pulling force for different side chain lengths, indicating the force f^{**} beyond which the backbone stretches on the length scales of a coarse-grained bead s^{**} in the implicit side chain model. (b) Deviation between the ESC and ISC model predictions: $\tilde{X}_{\rm ESC} = R_x/L$ as determined from the explicit side chain (ESC) model and $\tilde{X}_{\rm ISC}$ is the corresponding quantity determined from the implicit side chain (ISC) model. The vertical lines denote the location of f^{**} above which the ISC model no longer holds.

accessible and outside the range of most synthesized bottlebrushes.³²

We show that our proposed stretching mechanism is reflected by the molecular structure in our simulations by plotting the average bond orientation correlation $\langle \cos \theta(s) \rangle =$ $\langle \mathbf{u}_i \cdot \mathbf{u}_{i+s} \rangle$ as a function of the number of monomers between the two bonds, s. In the absence of a pulling force, this bond orientation correlation exhibits a monotonic decay as the backbone orientation is lost, plotted in Figure S1 for a number of different side chains, $N_{\rm sc}$. Melt simulations in the literature²⁴ show that this quantity can be fitted to a double-exponential indicative of local and global persistence length behaviors in analogy to conformations in polyelectrolyte solutions. 91-93 We do not pursue fitting to these curves in view of the numerous difficulties encountered in the literature 84,94 in extracting a single persistence length but simply note that doubleexponential decay suggests different conformational statistics at large versus small s values.

When force is applied to bottlebrush polymers in simulation, this backbone bond-bond autocorrelation exhibits deviations from the no-force case, as shown in Figure 5a, at large values of s. These deviations become more significant as the force is increased and occur at lower values of s. To interpret these trends, we plot in Figure 5b the absolute value of the deviation $|\Delta\langle \cos \theta(s)\rangle|$ of the backbone bond-bond autocorrelation function $\langle \cos \theta(s) \rangle$ from the no-force case as f is increased for $N_{\rm sc}$ = 8. Plots of the same quantity for multiple values of $N_{\rm sc}$ are provided in the Supporting Information. In analogy to traditional tension blob concepts in scaling arguments for linear chain extension, 95 we identify a length scale (in terms of the number of backbone bonds) by the onset of divergence in the deviation curves when s gets beyond a critical value, s*. We attribute s* to a length scale above which the bottlebrush backbone is extended and below which it behaves similar to the f = 0 curve. A quantitative value of s^* is determined as the intersection between a linear fit to the intermediate-s deviation

in $\langle \cos \theta(s) \rangle$ and the f=0 curve, shown for $N_{sc}=8$ in Figure 5(b). We find this to be the most reliable method for determining s^* as this intermediate-s regime is clearly visible on all plots of $|\Delta \langle \cos \theta(s) \rangle|$ versus s. We plot s^* as a function of f for different side chain lengths in Figure 6a. A decrease in s^* with an increase in the force indicates that the backbone is getting stretched on progressively smaller length scales. A power-law fit of the form $s^* \approx f^a$ to the data in Figure 6a shows α to increase with N_{sc} from $\alpha=-0.98$ at $N_{sc}=2$ to $\alpha=-0.62$ at $N_{sc}=20$. We note that this appears inconsistent with the standard scaling argument for linear polymers $f \approx k_B T/D$, 17,95 which we attribute to the increasing importance of the bottlebrush molecular structure as s^* decreases with force.

The ISC model predictions will start to deviate from the ESC model predictions when the backbone stretches on the length scale of a coarse-grained bead in the ISC model, so we choose to identify a $s^{**} = N_{sc}$ as the key value of s^* that reflects this length scale. The pulling force f^{**} corresponding to s** thus provides an upper bound on the allowable pulling force to maintain the validity of the ISC model. We plot s^* as a function of f for different side chain lengths in Figure 6a and indicate f^{**} on the plot. We plot this value f^{**} as vertical lines in absolute deviations of the relative extensions $|\tilde{X}_{ESC} - \tilde{X}_{ISC}|$ where $\tilde{X} = \langle R_x \rangle / L$) in Figure 6b between the ESC and ISC models as well as in Figure 2a, indicating that the ISC model ceases to hold beyond this value of the force. Indeed, there is qualitative agreement between where we indicate f^{**} and where deviations from the ISC become significant. This force f** also corresponds to significant deviations of the quantity $|\Delta\langle\cos\theta(s)\rangle|$ in the low-s limit. Since we attribute the linear increase in $|\Delta\langle \cos \theta(s)\rangle|$ at intermediate s to force-driven backbone extension, we attribute the emergence of this low-s plateau to rearrangements in the side-chain degrees of freedom that occur when the bottlebrush backbone is stretched. Thus, both the backbone distortion and the corresponding side-chain rearrangements occur on length scales below the coarsegrained bead of the ISC model, and the ISC model no longer captures the force-extension behavior of bottlebrush polymers.

4. CONCLUSIONS

In conclusion, we used simulation to study the stretching behavior of bottlebrush polymers using both an explicit side chain model and an implicit side chain model based on a wormlike cylinder representation. We observe a low-force regime in which the coarse-grained model is sufficient to explain bottlebrush elasticity, which can extend into the nonlinear regime of force-extension. At high forces, this coarsegrained picture of bottlebrush structure is insufficient, and internal molecular degrees of freedom become stretched. Backbone bond orientation correlations indicate that this stretching can be attributed to backbone stretching at length scales below that of the coarse-grained bead; this divergence occurs at lower forces as $N_{\rm sc}$ increases in part due to the implicit side chain model using fewer and fewer beads to represent the decreasingly cylindrical bottlebrush structure and correspondingly to the increased disparity between the contour lengths of the bottlebrush shape and the backbone. Forceinduced structural changes as evidenced from the backbone bond-bond autocorrelation curves explain the molecular origin of the force-dependent persistence length observed in the experimental studies discussed in the Introduction. Ultimately, this establishes the limits within which this coarse-grained approach to bottlebrush structure can be used

and where explicit side chain details may need to be considered. This poses limitations to the modeling of bottlebrush systems where strong forces are placed on the polymers, such as in soft elastomers or processing flows. 47,48,57,58

We hypothesize that empirical corrections may be able to further extend this implicit side chain model if, e.g., a stiff spring was used to represent backbone stretching; however, it remains to be seen if this can be predicted a priori and has any advantage over direct parameterization from simulation forceextension curves. In addition, there remains other molecular attributes of bottlebrush systems, such as the side-chain grafting density or bottlebrush concentration that represent areas of interest for future studies. We anticipate that this implicit side-chain representation will be useful in modeling bottlebrush materials where explicit side-chain models are computationally expensive. Incorporating these molecular features of bottlebrush elasticity will likely be key to predicting the properties of bottlebrush elastomers, 47,48 self-assembled block bottlebrush polymers, 57,58 and flowing bottlebrush solutions⁵⁸ and may enable comparison of this two-regime picture to experimental observables.

ASSOCIATED CONTENT

Solution Supporting Information

The Supporting Information is available free of charge at https://pubs.acs.org/doi/10.1021/acs.macromol.0c01184.

Backbone autocorrelation function for various side chain lengths and pulling forces and their deviation from the respective curves in the absence of a pulling force (PDF)

AUTHOR INFORMATION

Corresponding Author

Charles E. Sing — Department of Chemical and Biomolecular Engineering, University of Illinois at Urbana-Champaign, Urbana, Illinois 61801, United States; ocid.org/0000-0001-7231-2685; Email: cesing@illinois.edu

Author

Sarit Dutta — Department of Chemical and Biomolecular Engineering, University of Illinois at Urbana-Champaign, Urbana, Illinois 61801, United States; orcid.org/0000-0002-6197-7881

Complete contact information is available at: https://pubs.acs.org/10.1021/acs.macromol.0c01184

Notes

The authors declare no competing financial interest.

ACKNOWLEDGMENTS

This work was supported by the National Science Foundation under DMREF Award no. DMR-1727605. The authors thank Simon Rogers, Damien Guironnet, Ying Diao, Tianyuan Pan, Matthew Wade, Dylan Walsh, and Bijal Patel for intellectual discussions regarding this work.

REFERENCES

- (1) Xie, G.; Martinez, M. R.; Olszewski, M.; Sheiko, S. S.; Matyjaszewski, K. Molecular bottlebrushes as novel materials. *Biomacromolecules* **2019**, 20, 27–54.
- (2) Sveinbjörnsson, B. R.; Weitekamp, R. A.; Miyake, G. M.; Xia, Y.; Atwater, H. A.; Grubbs, R. H. Rapid selfassembly of brush block

- copolymers to photonic crystals. Proc. Natl. Acad. Sci. U. S. A. 2012, 109, 14332–14336.
- (3) Saito, Y.; Kikuchi, M.; Jinbo, Y.; Narumi, A.; Kawaguchi, S. Determination of the chain stiffness parameter of molecular rod brushes consisting of a polymethacrylate main chain and poly(n-hexyl isocyanate) side chains. *Macromolecules* **2015**, *48*, 8971–8979.
- (4) Liberman-Martin, A. L.; Chu, C. K.; Grubbs, R. H. Application of bottlebrush block copolymers as photonic crystals. *Macromol. Rapid Commun.* **2017**, *38*, 1700058.
- (5) Aluculesei, A.; Pipertzis, A.; Piunova, V. A.; Miyake, G. M.; Floudas, G.; Fytas, G.; Grubbs, R. H. Thermomechanical behavior and local dynamics of dendronized block copolymers and constituent homopolymers. *Macromolecules* **2015**, *48*, 4142–4150.
- (6) Sun, F.; Sheiko, S. S.; Möller, M.; Beers, K.; Matyjaszewski, K. Conformational switching of molecular brushes in response to the energy of interaction with the substrate. *J. Phys. Chem. A* **2004**, *108*, 9682–9686.
- (7) Xu, H.; Sun, F. C.; Shirvanyants, D. G.; Rubinstein, M.; Shabratov, D.; Beers, K. L.; Matyjaszewski, K.; Sheiko, S. S. Molecular pressure sensors. *Adv. Mater.* **2007**, *19*, 2930–2934.
- (8) Arrington, K. J.; Radzinski, S. C.; Drummey, K. J.; Long, T. E.; Matson, J. B. Reversibly cross-linkable bottlebrush polymers as pressure-sensitive adhesives. *ACS Appl. Mater. Interfaces* **2018**, *10*, 26662–26668.
- (9) Lee, H.-i.; Boyce, J. R.; Nese, A.; Sheiko, S. S.; Matyjaszewski, K. Ph-induced conformational changes of loosely grafted molecular brushes containing poly(acrylic acid) side chains. *Polymer* **2008**, *49*, 5490–5496.
- (10) Lee, H.-I.; Pietrasik, J.; Sheiko, S. S.; Matyjaszewski, K. Stimuli-responsive molecular brushes. *Prog. Polym. Sci.* **2010**, *35*, 24–44.
- (11) Birshtein, T. M.; Borisov, O. V.; Zhulina, Y. B.; Khokhlov, A. R.; Yurasova, T. A. Conformations of comb-like macromolecules. *Polym. Sci. U.S.S.R.* **1987**, *29*, 1293–1300.
- (12) Fredrickson, G. H. Surfactant-induced lyotropic behavior of flexible polymer solutions. *Macromolecules* **1993**, *26*, 2825–2831.
- (13) Lecommandoux, S.; Chécot, F.; Borsali, R.; Schappacher, M.; Deffieux, A.; Brûlet, A.; Cotton, J. P. Effect of dense grafting on the backbone conformation of bottlebrush polymers: determination of the persistence length in solution. *Macromolecules* **2002**, *35*, 8878–8881.
- (14) Feuz, L.; Leermakers, F. A. M.; Textor, M.; Borisov, O. Bending rigidity and induced persistence length of molecular bottle brushes: a self-consistent-field theory. *Macromolecules* **2005**, *38*, 8891–8901.
- (15) Subbotin, A.; de Jong, J.; ten Brinke, G. Spontaneous bending of 2d molecular bottle-brush. *Eur. Phys. J. E: Soft Matter Biol. Phys.* **2006**, 20, 99–108.
- (16) Borisov, O. V.; Zhulina, E. B.; Birshtein, T. M. Persistence length of dendritic molecular brushes. *ACS Macro Lett.* **2012**, *1*, 1166–1169.
- (17) Zhulina, E. B.; Sheiko, S. S.; Borisov, O. V. Solution and melts of barbwire bottlebrushes: Hierarchical structure and scale-dependent elasticity. *Macromolecules* **2019**, 1671.
- (18) Rouault, Y.; Borisov, O. V. Comb-branched polymers: monte carlo simulation and scaling. *Macromolecules* **1996**, *29*, 2605–2611.
- (19) Khalatur, P. G.; Shirvanyanz, D. G.; Starovoitova, N. Y.; Khokhlov, A. R. Conformational properties and dynamics of molecular bottle-brushes: A cellular-automaton-based simulation. *Macromol. Theory Simul.* **2000**, *9*, 141–155.
- (20) Yethiraj, A. A monte carlo simulation study of branched polymers. J. Chem. Phys. 2006, 125, 204901–204910.
- (21) Hsu, H.-P.; Paul, W.; Binder, K. Structure of bottle-brush polymers in solution: A monte carlo test of models for the scattering function. *J. Chem. Phys.* **2008**, *129*, 204904–204912.
- (22) Hsu, H.-P.; Paul, W.; Rathgeber, S.; Binder, K. Characteristic length scales and radial monomer density profiles of molecular bottle-brushes: Simulation and experiment. *Macromolecules* **2010**, *43*, 1592–1601.
- (23) Theodorakis, P. E.; Paul, W.; Binder, K. Pearl-necklace structures of molecular brushes with rigid backbone under poor

- solvent conditions: A simulation study. J. Chem. Phys. 2010, 133, 104901–104910.
- (24) Cao, Z.; Carrillo, J.-M. Y.; Sheiko, S. S.; Dobrynin, A. V. Computer simulations of bottle brushes: From melts to soft networks. *Macromolecules* **2015**, *48*, 5006–5015.
- (25) Hsu, H.-P.; Paul, W.; Binder, K. Understanding the multiple length scales describing the structure of bottle-brush polymers by monte carlo simulation methods. *Macromol. Theory Simul.* **2011**, 20, 510–525.
- (26) Daniel, W. F. M.; Burdyńska, J.; Vatankhah-Varnoosfaderani, M.; Matyjaszewski, K.; Paturej, J.; Rubinstein, M.; Dobrynin, A. V.; Sheiko, S. S. Solvent-free, supersoft and superelastic bottlebrush melts and networks. *Nat. Mater.* **2016**, *15*, 183–189.
- (27) Chatterjee, D.; Vilgis, T. A. Scaling laws of bottle-brush polymers in dilute solutions. *Macromol. Theory Simul.* **2016**, 25, 518–523.
- (28) Paturej, J.; Sheiko, S. S.; Panyukov, S.; Rubinstein, M. Molecular structure of bottlebrush polymers in melts. *Sci. Adv.* **2016**, 2, No. e1601478.
- (29) Paturej, J.; Kreer, T. Hierarchical excluded volume screening in solutions of bottlebrush polymers. *Soft Matter* **2017**, *13*, 8534–8541.
- (30) Lyubimov, I.; Wessels, M. G.; Jayaraman, A. Molecular dynamics simulation and prism theory study of assembly in solutions of amphiphilic bottlebrush block copolymers. *Macromolecules* **2018**, *51*, 7586–7599.
- (31) Wessels, M. G.; Jayaraman, A. Molecular dynamics simulation study of linear, bottlebrush, and star-like amphiphilic block polymer assembly in solution. *Soft Matter* **2019**, *15*, 3987–3998.
- (32) Dutta, S.; Wade, M. A.; Walsh, D. J.; Guironnet, D.; Rogers, S. A.; Sing, C. E. Dilute solution structure of bottlebrush polymers. *Soft Matter* **2019**, *15*, 2928–2941.
- (33) Wintermantel, M.; Gerle, M.; Fischer, K.; Schmidt, M.; Wataoka, I.; Urakawa, H.; Kajiwara, K.; Tsukahara, Y. Molecular bottlebrushes. *Macromolecules* **1996**, 29, 978–983.
- (34) Kawaguchi, S.; Akaike, K.; Zhang, Z.-M.; Matsumoto, H.; Ito, K. Water soluble bottlebrushes. *Polym. J.* **1998**, *30*, 1004–1007.
- (35) Terao, K.; Takeo, Y.; Tazaki, M.; Nakamura, Y.; Norisuye, T. Polymacromonomer consisting of polystyrene. Light scattering characterization in cyclohexane. *Polym J.* **1999**, *31*, 193–198.
- (36) Terao, K.; Nakamura, Y.; Norisuye, T. Solution properties of polymacromonomers consisting of polystyrene. 2. Chain dimensions and stiffness in cyclohexane and toluene. *Macromolecules* **1999**, 32, 711–716.
- (37) Rathgeber, S.; Pakula, T.; Wilk, A.; Matyjaszewski, K.; Beers, K. L. On the shape of bottle-brush macromolecules: Systematic variation of architectural parameters. *J. Chem. Phys.* **2005**, *122*, 124904–124914.
- (38) Amitani, K.; Terao, K.; Nakamura, Y.; Norisuye, T. Small-angle x-ray scattering from polystyrene polymacromonomers in cyclohexane. *Polym. J.* **2005**, *37*, 324–331.
- (39) Rathgeber, S.; Pakula, T.; Wilk, A.; Matyjaszewski, K.; Lee, H.-I.; Beers, K. L. Bottle-brush macromolecules in solution: Comparison between results obtained from scattering experiments and computer simulations. *Polymer* **2006**, *47*, 7318–7327.
- (40) Sugiyama, M.; Nakamura, Y.; Norisuye, T. Dilute-solution properties of polystyrene polymacromonomer having side chains of over 100 monomeric units. *Polym. J.* **2007**, *40*, 109–115.
- (41) Pesek, S. L.; Li, X.; Hammouda, B.; Hong, K.; Verduzco, R. Small-angle neutron scattering analysis of bottlebrush polymers prepared via grafting-through polymerization. *Macromolecules* **2013**, 46, 6998–7005.
- (42) Pesek, S. L.; Xiang, Q.; Hammouda, B.; Verduzco, R. Smallangle neutron scattering analysis of bottlebrush backbone and side chain flexibility. *J. Polym. Sci., Part B: Polym. Phys.* **2017**, *55*, 104–111.
- (43) Namba, S.; Tsukahara, Y.; Kaeriyama, K.; Okamoto, K.; Takahashi, M. Bulk properties of multibranched polystyrenes from polystyrene macromonomers: Rheological behavior I. *Polymer* **2000**, 41, 5165–5171.

- (44) Sheiko, S. S.; Sumerlin, B. S.; Matyjaszewski, K. Cylindrical molecular brushes: Synthesis, characterization, and properties. *Prog. Polym. Sci.* **2008**, *33*, 759–785.
- (45) Rzayev, J. Molecular bottlebrushes: New opportunities in nanomaterials fabrication. ACS Macro Lett. 2012, 1, 1146–1149.
- (46) Xu, H.; Shirvanyants, D.; Beers, K. L.; Matyjaszewski, K.; Dobrynin, A. V.; Rubinstein, M.; Sheiko, S. S. Molecular visualization of conformation-triggered flow instability. *Phys. Rev. Lett.* **2005**, *94*, 237801.
- (47) Vatankhah-Varnoosfaderani, M.; Daniel, W. F. M.; Zhushma, A. P.; Li, Q.; Morgan, B. J.; Matyjaszewski, K.; Armstrong, D. P.; Spontak, R. J.; Dobrynin, A. V.; Sheiko, S. S. Bottlebrush elastomers: A new platform for freestanding electroactuation. *Adv. Mater.* **2017**, 29, 1604209.
- (48) Vatankhah-Varnosfaderani, M.; Daniel, W. F. M.; Everhart, M. H.; Pandya, A. A.; Liang, H.; Matyjaszewski, K.; Dobrynin, A. V.; Sheiko, S. S. Mimicking biological stress—strain behaviour with synthetic elastomers. *Nature* **2017**, *549*, 497—501.
- (49) Liang, H.; Sheiko, S. S.; Dobrynin, A. V. Supersoft and hyperelastic polymer networks with brushlike strands. *Macromolecules* **2018**, *51*, 638–645.
- (50) Jacobs, M.; Liang, H.; Dashtimoghadam, E.; Morgan, B. J.; Sheiko, S. S.; Dobrynin, A. V. Nonlinear elasticity and swelling of comb and bottlebrush networks. *Macromolecules* **2019**, 5095.
- (51) Sheiko, S. S.; Sun, F. C.; Randall, A.; Shirvanyants, D.; Rubinstein, M.; Lee, H.-I.; Matyjaszewski, K. Adsorption-induced scission of carbon–carbon bonds. *Nature* **2006**, 440, 191–194.
- (52) Panyukov, S.; Zhulina, E. B.; Sheiko, S. S.; Randall, G. C.; Brock, J.; Rubinstein, M. Tension amplification in molecular brushes in solutions and on substrates. *J. Phys. Chem. B* **2009**, *113*, 3750–3768.
- (53) Chae, C.-G.; Yu, Y.-G.; Seo, H.-B.; Kim, M.-J.; Grubbs, R. H.; Lee, J.-S. Experimental formulation of photonic crystal properties for hierarchically self-assembled poss—bottlebrush block copolymers. *Macromolecules* **2018**, *51*, 3458—3466.
- (54) Wessels, M. G.; Jayaraman, A. Self-assembly of amphiphilic polymers of varying architectures near attractive surfaces. *Soft Matter* **2020**, *16*, 623–633.
- (55) Abbasi, M.; Faust, L.; Riazi, K.; Wilhelm, M. Linear and extensional rheology of model branched polystyrenes: From loosely grafted combs to bottlebrushes. *Macromolecules* **2017**, *50*, 5964–5977.
- (56) López-Barrón, C. R.; Shivokhin, M. E. Extensional strain hardening in highly entangled molecular bottlebrushes. *Phys. Rev. Lett.* **2019**, *122*, No. 037801.
- (57) Wade, M. A.; Walsh, D.; Lee, J. C.-W.; Kelley, E.; Weigandt, K.; Guironnet, D.; Rogers, S. A. Color, structure, and rheology of a diblock bottlebrush copolymer solution. *Soft Matter* **2020**, *16*, 4919–4931.
- (58) Patel, B. B.; Walsh, D. J.; Kim, D. H.; Kwok, J.; Lee, B.; Guironnet, D.; Diao, Y. Tunable structural color of bottlebrush block copolymers through direct-write 3D printing from solution. *Sci. Adv.* **2020**, *6*, No. eaaz7202.
- (59) Pelras, T.; Mahon, C. S.; Müllner, M. Synthesis and applications of compartmentalised molecular polymer brushes. *Angew. Chem. Int. Ed.* **2018**, *57*, 6982–6994.
- (60) Pincus, P. Excluded volume effects and stretched polymer chains. *Macromolecules* **1976**, *9*, 386–388.
- (61) Rocha, M. S.; Storm, I. M.; Bazoni, R. F.; Ramos, É. B.; Hernandez-Garcia, A.; Cohen Stuart, M. A.; Leermakers, F.; de Vries, R. Force and scale dependence of the elasticity of self-assembled DNA bottle brushes. *Macromolecules* **2017**, *51*, 204–212.
- (62) Marko, J. F.; Siggia, E. D. Stretching DNA. *Macromolecules* **1995**, 28, 8759–8770.
- (63) Berezney, J. P.; Marciel, A. B.; Schroeder, C. M.; Saleh, O. A. Scale-dependent stiffness and internal tension of a model brush polymer. *Phys. Rev. Lett.* **2017**, *119*, 127801.
- (64) Innes-Gold, S. N.; Berezney, J. P.; Saleh, O. A. Single-molecule mechanical measurements of the hyaluronan-aggrecan bottlebrush. *Biophysical Journal* **2020**, 200a.

- (65) Jacobson, D. R.; McIntosh, D. B.; Stevens, M. J.; Rubinstein, M.; Saleh, O. A. Single-stranded nucleic acid elasticity arises from internal electrostatic tension. *Proc. Natl. Acad. Sci. U. S. A.* **2017**, *114*, 5095–5100.
- (66) Müllner, M.; Müller, A. H. E. Cylindrical polymer brushes anisotropic building blocks, unimolecular templates and particulate nanocarriers. *Polymer* **2016**, *98*, 389–401.
- (67) Morrison, G.; Hyeon, C.; Toan, N. M.; Ha, B.-Y.; Thirumalai, D. Stretching homopolymers. *Macromolecules* **2007**, *40*, 7343–7353.
- (68) Saleh, O. A.; McIntosh, D. B.; Pincus, P.; Ribeck, N. Nonlinear low-force elasticity of singlestranded DNA molecules. *Phys. Rev. Lett.* **2009**, *102*, 477.
- (69) Hsu, H.-P.; Binder, K. Stretching semiflexible polymer chains: Evidence for the importance of excluded volume effects from monte carlo simulation. *J. Chem. Phys.* **2012**, *136*, No. 024901.
- (70) Stevens, M. J.; McIntosh, D. B.; Saleh, O. A. Simulations of stretching a strong, flexible polyelectrolyte: Using long chains to access the pincus scaling regime. *Macromolecules* **2013**, *46*, 6369–6373.
- (71) Li, X.; Schroeder, C. M.; Dorfman, K. D. Modeling the stretching of wormlike chains in the presence of excluded volume. *Soft Matter* **2015**, *11*, 5947–5954.
- (72) Walsh, D. J.; Guironnet, D. Macromolecules with programmable shape, size, and chemistry. *Proc. Natl. Acad. Sci. U. S. A.* **2019**, 116, 1538–1542.
- (73) Walsh, D. J.; Dutta, S.; Sing, C. E.; Guironnet, D. Engineering of molecular geometry in bottlebrush polymers. *Macromolecules* **2019**, 52, 4847–4857.
- (74) Dutta, S.; Pan, T.; Sing, C. E. Bridging simulation length scales of bottlebrush polymers using a wormlike cylinder model. *Macromolecules* **2019**, *52*, 4858–4874.
- (75) Terao, K.; Hokajo, T.; Nakamura, Y.; Norisuye, T. Solution properties of polymacromonomers consisting of polystyrene. 3. Viscosity behavior in cyclohexane and toluene. *Macromolecules* **1999**, 32, 3690–3694.
- (76) Hokajo, T.; Terao, K.; Nakamura, Y.; Norisuye, T. Solution properties of polymacromonomers consisting of polystyrene v. Effect of side chain length on chain stiffness. *Polym. J.* **2001**, 33, 481–485.
- (77) Hokajo, T.; Hanaoka, Y.; Nakamura, Y.; Norisuye, T. Translational diffusion coefficient of polystyrene polymacromonomers. Dependence on side-chain length. *Polym. J.* **2005**, *37*, 529–534.
- (78) Kikuchi, M.; Lien, L. T. N.; Narumi, A.; Jinbo, Y.; Izumi, Y.; Nagai, K.; Kawaguchi, S. Conformational properties of cylindrical rod brushes consisting of a polystyrene main chain and poly(n-hexyl isocyanate) side chains. *Macromolecules* **2008**, *41*, 6564–6572.
- (79) Inoue, K.; Yamamoto, S.; Nakamura, Y. Dilute solution properties of a polymacromonomer consisting of a polystyrene main chain with polyisoprene side chains. Relation of molecular parameters to polymer segment interactions. *Macromolecules* **2013**, *46*, 8664–8670.
- (80) Kikuchi, M.; Nakano, R.; Jinbo, Y.; Saito, Y.; Ohno, S.; Togashi, D.; Enomoto, K.; Narumi, A.; Haba, O.; Kawaguchi, S. Graft density dependence of main chain stiffness in molecular rod brushes. *Macromolecules* **2015**, *48*, 5878–5886.
- (81) Kikuchi, M.; Takahara, A.; Kawaguchi, S. Dimensional characterizations from rod stars to brushes of polymers with a low degree of polymerization. *Macromolecules* **2016**, *50*, 324–331.
- (82) Yamakawa, H.; Yoshizaki, T. Helical wormlike chains in polymer solutions, 2nd ed.; SpringerVerlag: Berlin, Heidelberg, 2016.
- (83) Fischer, K.; Schmidt, M. Solvent-induced length variation of cylindrical brushes. *Macromol. Rapid Commun* **2001**, 22, 787–791.
- (84) Theodorakis, P. E.; Hsu, H.-P.; Paul, W.; Binder, K. Computer simulation of bottle-brush polymers with flexible backbone: Good solvent versus theta solvent conditions. *J. Chem. Phys.* **2011**, *135*, 164903.
- (85) Terao, K.; Hayashi, S.; Nakamura, Y.; Norisuye, T. Solution properties of polymacromonomers consisting of polystyrene. *Polym. Bull.* **2000**, *44*, 309–316.

- (86) Schellman, J. A. Flexibility of DNA. *Biopolymers* **1974**, 13, 217–226.
- (87) Tree, D. R.; Muralidhar, A.; Doyle, P. S.; Dorfman, K. D. Is DNA a good model polymer? *Macromolecules* **2013**, *46*, 8369–8382.
- (88) Saleh, O. A. Perspective: Single polymer mechanics across the force regimes. *J. Chem. Phys.* **2015**, *142*, 194902.
- (89) de Gennes, P. G. Dynamics of entangled polymer solutions I. The rouse model. *Macromolecules* **1976**, *9*, 587–593.
- (90) Nakamura, Y.; Norisuye, T. Brush-like polymers. In Soft Matter Characterization; R, B., R, P., Eds.; 2008; pp 235–286.
- (91) Manghi, M.; Netz, R. R. Variational theory for a single polyelectrolyte chain revisited. *Eur. Phys. J. E: Soft Matter Biol. Phys.* **2004**, *14*, 67–77.
- (92) Gubarev, A.; Carrillo, J.-M. Y.; Dobrynin, A. V. Scale-dependent electrostatic stiffening in biopolymers. *Macromolecules* **2009**, 42, 5851–5860.
- (93) Carrillo, J.-M. Y.; Dobrynin, A. V. Polyelectrolytes in salt solutions: Molecular dynamics simulations. *Macromolecules* **2011**, *44*, 5798–5816.
- (94) Hsu, H.-P.; Paul, W.; Binder, K. Standard definitions of persistence length do not describe the local "intrinsic" stiffness of real polymer chains. *Macromolecules* **2010**, *43*, 3094–3102.
- (95) de Gennes, P. G. Scaling Concepts in Polymer Physics; Cornell University Press, 1979.